

Direct Torque and Flux Controlled Space Vector Modulated (DTFC-SVM) Based on Fuzzy Logic Controller for Line-Start Permanent Magnet Synchronous and Permanent Magnet Synchronous Machines

Mohsen Hosseinzadeh Soreshjani*, Ahmad Ghafari**, Mortaza Haghparast*

*Department of Shahrekord University, Shahrekord, Iran

**Department of Engineering, Shahid-Chamran University, Ahvaz, Iran. e-mail:

E-mail: hosseinzadeh.ieee@yahoo.com, ahmad_ghafari@yahoo.com, m_haghparast@hotmail.com

Abstract: In this paper, Direct Torque and Flux Control (DTFC) method based on Space Vector Modulation (SVM) technique is designed for a Line-Start Permanent Magnet Synchronous Motor (LSPMSM) and its equal Permanent Magnet Synchronous Motor (PMSM). In addition, the LSPMSM is designed using finite element analysis. Moreover, the same Fuzzy Logic Controllers (FLCs) with minimum simple triangle membership functions and reduced rule bases are designed and used. In order to present a thorough comparison, the same conditions are tested for both motors. Simulation results from MATLAB/Simulink software are presented for independent control of torque and flux motor parameters, and the advantages of the proposed method for the LSPMSM over the PMSM are analyzed.

Keywords: Line-Start Permanent Magnet Synchronous Motor (LSPMSM), Permanent Magnet Synchronous Motor (PMSM), Direct Torque Flux Control (DTFC), Fuzzy Logic Controller (FLC).

1. INTRODUCTION

In the past, DC motors were widely used for speed control applications. However, thanks to recent advances in the power electronic devices, AC motors are now extensively employed in adjustable speed drive applications (Ferreira *et al.*, 2011; deAlmeida *et al.*, 2011; Vas, 1998). In this regard, Induction Motors (IMs) have widely been applied in different industries, because of their simplicity, ruggedness, reliability, and volume manufacturing. However, slip and rotor copper losses of IMs reduce their efficiency and Power Factor (PF) significantly (deAlmeida *et al.*, 2011; Vas, 1998; CheeMun, 1997; Melfi *et al.*, 2009).

The fixed synchronous speed with a high desired level of efficiency and PF is provided for synchronous motors. Nevertheless, they have a higher cost and a more complex structure rather than induction motors. For this reason, Permanent Magnet (PM) materials are employed in synchronous motors, and the decreasing price along with improved performances of permanent magnet materials make PMSMs far more interesting than before (Vas, 1998; CheeMun, 1997; Melfi *et al.*, 2009; Melfi *et al.*, 2008).

In the asynchronous region, PMSMs produce an oscillating torque which is not able to accelerate the rotor. In other words, PMSMs are not able to start with a fixed voltage frequency, and for this reason, LSPMSMs which are synchronous hybrid PM/reluctance high-efficient motors are recommended (Kurihara and Rahman, 2004; Isfahani, Vaez-Zadeh, 2009; Marcic *et al.*, 2008). In LSPMSMs, rotor cage and PM materials provide the induction starting capability and synchronous torque, respectively. LSPMSMs are introduced as suitable substitutes for induction motors and

PMSMs. Different researches have recently evaluated every aspect of LSPMSMs and equal induction motors (Fei *et al.*, 2009; Kahrisangi *et al.*, 2012; Stumberger *et al.*, 2012; Marcic *et al.*, 2012). LSPMSMs are also being developed for various applications, especially electrical drive ones (Marcic *et al.*, 2012; Taravat *et al.*, 2012), however, any known closed-loop control system for three-phase LSPMSMs has not been designed yet. In reference (Taravat *et al.*, 2012), a sensor-less vector control has been designed only for a single-phase LSPMSM. The DTFC, which is robust against system variations, provides a fast and decoupled response, and thus it has been much progress, developed, and improved recently (Vas, 1998; Yongchang *et al.*, 2012; Elbadsai *et al.*, 2013; Uddin and Hafeez, 2012; Jidin *et al.*, 2012; Yongchang and Jianguo, 2011).

Application of artificial intelligence methods in electrical drives is interesting and motivating, as well. Among these methods, fuzzy systems are designed based on human knowledge for unknown, nonlinear, or complicated systems to present a robust response (Schwartz *et al.*, 1994). Thus, in the past three decades, they have replaced conventional controllers in many applications and industries.

The main contribution of this paper is to design the well-known DTFC-SVM method using the FLC for a three-phase LSPMSM. In addition, the performance of this method is analysed and compared with its equal PMSM, and various conditions are tested to present an in-depth comparative analysis. Therefore, the fuzzy controller is designed here as a simple and robust control scheme. Simulation results from MATLAB/ Simulink software confirm the method. The results also show that, particularly for the LSPMSM, this

method has a distinctive impact on the dynamic and steady-state performance.

This paper is organized as follows. Section 2 provides modelling and description of PMSMs and LSPMSMs principles along with their designing issues. Section 3 is devoted to design a simple DTFC-SVM method and FLC for both PMSM and LSPMSM. In section 4, to verify the presented control system, DTFC-SVM of both motors are simulated in the MATLAB/SIMULINK software under the same conditions.

2. GENERAL DESCRIPTION

Since LSPMSMs include a squirrel cage rotor of induction motors and permanent magnet segments, a prototype of the original model along with rotor cross sections of induction motor and LSPMSM is shown in Figure 1. In general, their stator are completely the same. It is noticeable that LSPMSMs unite the merits of induction motors (robust construction with respect to disturbance and line-starting ability) and PMSMs (high PF, efficiency, and torque per unit current density). Although their self-starting capability for fixed supply voltages is one of the most frequently cited features of the LSPMSMs over the PMSMs, they are hereby compared when supplied from the same voltage source inverters. Therefore, models of these motors are reviewed as follows.

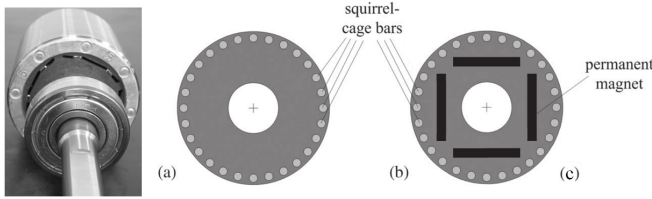


Fig. 1. (a). A prototype of the original model, and rotor cross sections of (b). Induction motor, (c). LSPMSM.

2.1 PMSM Model

A three-phase PMSM, is modelled as follows (deAlmeida *et al.*, 2011):

$$\begin{cases} \lambda_{qs}^r = (L_{ls} + L_{mq})i_{qs}^r \\ \lambda_{ds}^r = (L_{ls} + L_{md})i_{ds}^r + L_{md}i_m^r = (L_{ls} + L_{md})i_{ds}^r + \lambda_m^r \\ \lambda_{0s}^r = L_{ls}i_{0s}^r \end{cases} \quad (1)$$

$$\begin{cases} V_{qs}^r = r_s i_{qs}^r + \omega_m \lambda_{ds}^r + p \lambda_{qs}^r \\ V_{ds}^r = r_s i_{ds}^r - \omega_m \lambda_{qs}^r + p \lambda_{ds}^r \\ V_{0s}^r = r_s i_{0s}^r + p \lambda_{0s}^r \end{cases} \quad (2)$$

where the direct, quadratic, and zero (d - q - 0) axes stator variables (V_{ds}^r , V_{qs}^r , V_{0s}^r), (i_{ds}^r , i_{qs}^r , i_{0s}^r), and (λ_{ds}^r , λ_{qs}^r , λ_{0s}^r) are the stator voltage, current, and flux, respectively. The equivalent magnetizing flux and current of the permanent magnet referred to the stator side are i_m^r and λ_m^r . In addition, p is the derivative operator, and r_s and L_{ls} are the stator resistance and leakage- inductance, and L_{md} and L_{mq} are the magnetizing inductances of direct and quadratic axes, respectively. The

equivalent circuits, shown in Figure 2, are based on (1-2), and mechanical equations are expressed as:

$$\begin{cases} Jp\omega_m = T_e - T_{Load} - B\omega_m \\ T_e = \left(\frac{3}{2}\right)\left(\frac{P}{2}\right)\{\lambda_m^r i_{qs}^r + (L_{md} - L_{mq})i_{ds}^r i_{qs}^r\} = T_{exc} + T_{Rel} \end{cases} \quad (3)$$

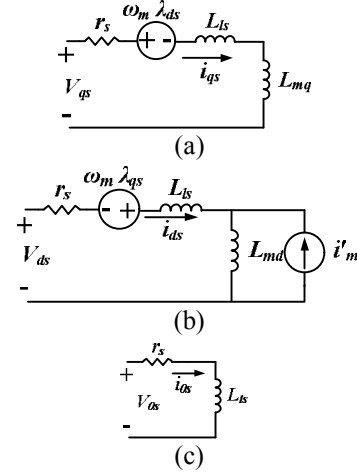


Fig. 2. Rotor reference frame of equivalent circuit of three-phase PMSM (a): q-axis, (b): d-axis, (c): 0-axis.

where ω_m and P are the angular speed and the pole numbers, respectively. Finally, T_e , T_{Load} , B , and J are the electromagnetic and load torques, friction coefficient, and moment of inertia, respectively. It is worthwhile to note that the generated electromagnetic torque of PMSM contains excitation torque (T_{exc}) and reluctance torque (T_{Rel}). The first term is produced thanks to the field of permanent magnet material, and the second one is formed, because of the saliency of the motor. Clearly, both terms are zero for an IM, since they are generated because of the permanent magnet materials.

2.2 LSPMSM Model

Because of the rotor cage windings, the equations of LSPMSM are obtained as:

$$\begin{cases} \lambda_{qs}^r = L_{ls}i_{qs}^r + L_{mq}(i_{qs}^r + i_{qr}^r) \\ \lambda_{ds}^r = L_{ls}i_{ds}^r + L_{md}(i_{ds}^r + i_{dr}^r) + L_{md}i_m^r \\ \lambda_{0s}^r = L_{ls}i_{0s}^r \end{cases} \quad (4)$$

$$\begin{cases} \lambda_{qr}^r = L'_{lr}i_{qr}^r + L_{mq}(i_{qs}^r + i_{qr}^r) \\ \lambda_{dr}^r = L'_{lr}i_{dr}^r + L_{md}(i_{ds}^r + i_{dr}^r) + L_{md}i_m^r \\ \lambda_{0r}^r = L'_{lr}i_{0r}^r \end{cases} \quad (5)$$

$$\begin{cases} V_{qs}^r = r_s i_{qs}^r + \omega_m \lambda_{ds}^r + p \lambda_{qs}^r \\ V_{ds}^r = r_s i_{ds}^r - \omega_m \lambda_{qs}^r + p \lambda_{ds}^r \\ V_{0s}^r = r_s i_{0s}^r + p \lambda_{0s}^r \end{cases} \quad (6)$$

$$\begin{cases} V_{qr}^r = r'_{qr} i_{qr}^r + p \lambda_{qr}^r = 0 \\ V_{dr}^r = r'_{dr} i_{dr}^r + p \lambda_{dr}^r = 0 \end{cases} \quad (7)$$

The equivalent circuits shown in Figure 3 are obtained based on (CheeMun, 1997, Melfi *et al.*, 2009; Melfi *et al.*, 2008; Kurihara and Rahman, 2004).

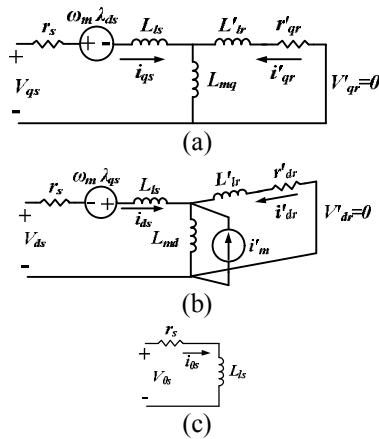


Fig. 3. Rotor reference frame of equivalent circuit of three-phase LSPMSM (a): q-axis, (b): d-axis, (c): 0-axis.

Again, its electromagnetic torque is expressed as:

$$\begin{cases} T_e = \left(\frac{3}{2}\right)\left(\frac{P}{2}\right)\left\{\lambda_m^r i_{qs}^r + \left((L_{md} - L_{mq})i_{ds}^r i_{qs}^r\right) + L_{md}i_{dr}^r i_{qs}^r - L_{mq}i_{qr}^r i_{ds}^r\right\} \\ T_e = T_{exc} + T_{Rel} + T_{ind} \end{cases} \quad (8)$$

The electromagnetic torque of LSPMSM is developed into three components: reluctance, excitation, and induction torques, and also it is expressed as (CheeMun, 1997):

$$T_e = \frac{3}{2} \frac{P}{2} (\lambda_{ds}^r i_{qs}^r - \lambda_{qs}^r i_{ds}^r) \quad (9)$$

Clearly, the flux of PM (λ'_m) is laid in the direct flux linkage, and (9) is completely equal to (3) which has been obtained for the PMSM, so they are hereby used for torque estimation.

2.3 LSPMSM and PMSM Design

In this section, an LSPMSM amended from an actual induction motor is designed. The induction motor is a 750 (W), 50 (Hz), 380 (v), four-pole, and three-phase squirrel cage motor, and it has an IEC80-4A frame size and a transversally laminated core. In addition, an equal PMSM is designed so that only electrical parameters of LSPMSM rotor can be infinitive and the other electrical parameters of the motor can be maintained. It provides the opportunity to evaluate the effect of rotor windings of the LSPMSM as well. Meanwhile, the same stators are here selected for both motors. Therefore, to present a better insight and comprison, the whole designed parameters of the afforementioned motors are listed in Table 1. However, different PMSMs can be designed, based on LSPMSM designing data. For instance, the same design data for both motors from Table 1 leads to a different PMSM.

Since the induction motor is an actual one, its electrical and mechanical parameters are available, but these parameters for LSPMSM and PMSM are computed using finite element analysis. Therefore, cross section of both designed motors

with the stator of the induction motor is shown in Figure 4. Moreover, the flux density in the air gap is shown in Figure 5. Meanwhile, the magnetic saliency ratio and PM flux of the designed LSPMSM are equal to 3.5 and 1.32 (Wb), respectively. Figures 6 and 7, respectively, show magnetic flux line distribution under different conditions for one pole of the designed motors.

Table 1. Design data of IM, LSPMSM, and PMSM.

| Public parameters | Motor Poles = 4 Stack length = 120 (mm) |
|-------------------------|---|
| Stator parameter | Stator bore = 35 (mm) Stator external radius = 62.5 (mm) Number of stator slots = 24 Number of winding turns per slot = 44 |
| IM rotor parameters | Rotor radius = 34.8 (mm) Rotor bore = 13 (mm) Number of rotor slots = 24 |
| LSPMSM rotor parameters | Rotor radius = 34.8 (mm) Rotor bore = 13 (mm) Number of rotor slots = 24 PM dimensions = [120, 33, 6] |
| PMSM rotor parameters | Rotor radius = 34.7 (mm) Rotor bore = 13 (mm) Number of rotor slots = 0 PM dimensions = [120, 29, 6] |
| PM material | NdFeB |

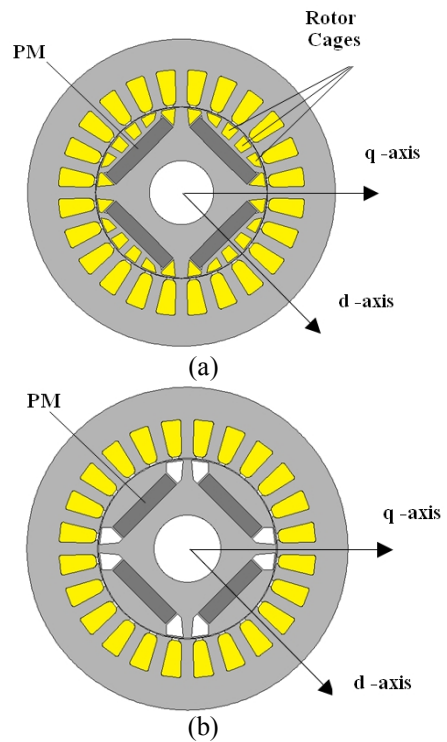


Fig. 4 A cross section of (a): designed LSPMSM, (b): designed PMSM.

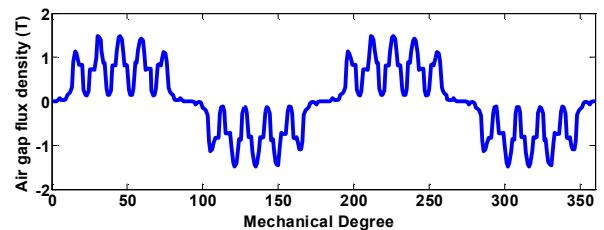


Fig. 5. Air gap flux density due to the permanent magnets in LSPMSM.

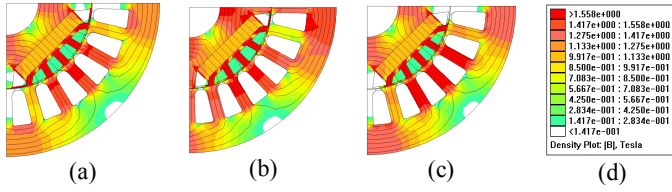


Fig. 6. Magnetic flux distribution for one pole of LSPMSM with: a) applying no current, applying current along b) q-axis and c) d-axis d) legend.

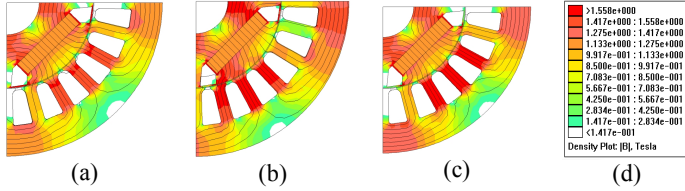


Fig. 7. Magnetic flux distribution for one pole of PMSM with: a) applying no current, applying current along b) q-axis and c) d-axis d) legend.

3. DIRECT TORQUE AND FLUX CONTROL

In this section, a well-known technique of DTFC based on SVM and a simple fuzzy controller are briefly discussed, and the reader is referred to (Vas, 1998) for more details. The FLC is hereby designed with minimum simple triangle membership functions and reduced rule bases. As the aim of this paper is to compare and test the effects of the DTFC-SVM scheme on LSPMSMs and PMSMs performance, intentionally a simple DTFC-SVM has been employed, and any of the known improved methods did not have been employed hereby.

3.1 DTFC SVM

Since DTFC method provides an accurate and fast decoupled control of the stator flux linkage and the electromagnetic torque with a fixed switching frequency (Vas, 1998), it has been improved extensively in the past decade (Vas, 1998; Yongchang *et al.*, 2012; Elbadi *et al.*, 2013; Uddin and Hafeez, 2012; Jidin *et al.*, 2012; Yongchang and Jianguo, 2011). In fact, the implementation of DTFC for LSPMSM and PMSM are completely the same. Therefore, a block diagram of the well-known DTFC-SVM scheme, which is applicable for both motors, is shown in Figure 8.

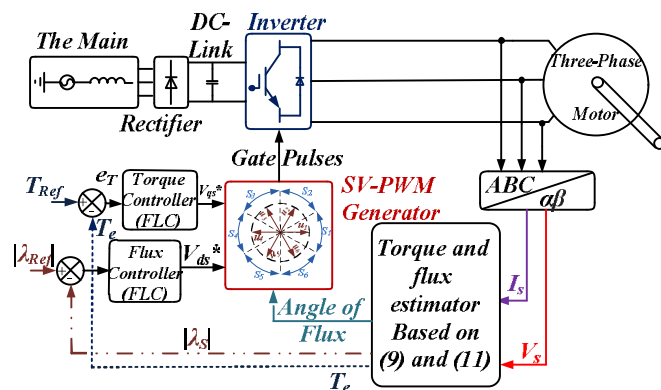


Fig. 8. A block diagram of DTFC-SVM for three-phase PMSM and LSPMSM drives.

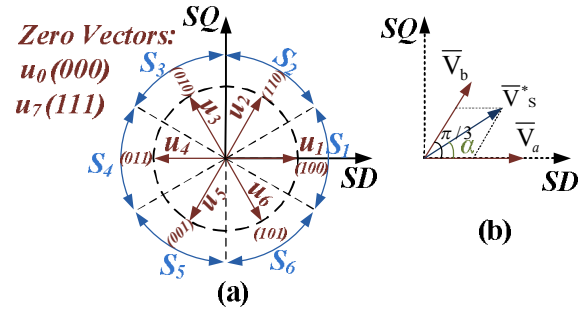


Fig. 9. (a): Inverter output voltage space vectors, (b): Reference vectors as a combination of adjacent vectors at sector 1.

Here, the space vector pulse width modulation technique, through the eight space vectors (V_0, V_1, \dots, V_7) illustrated in Figure 9 (a), is employed to optimize the switching signals. In each switching cycle ($T_s = 1/f_s$), as shown in Figure 9 (b), two nearest active vectors (\bar{V}_a and \bar{V}_b) and one zero vector are, respectively, selected at T_1 , T_2 , and T_0 duration, and they are determined as:

$$\begin{cases} T_1 = \frac{\sqrt{3}|\bar{V}_s^*|}{V_{dc} \cdot f_s} \left(\sin\left(\frac{\pi}{3} - \alpha + \frac{n-1}{3}\pi\right) \right) \\ T_2 = \frac{\sqrt{3}|\bar{V}_s^*|}{V_{dc} \cdot f_s} \left(\sin\left(\alpha - \frac{n-1}{3}\pi\right) \right) \\ T_0 = \frac{1}{f_s} - T_1 - T_2 \end{cases} \quad (10)$$

where α is the angle between \bar{V}_a and \bar{V}_s^* vectors. Equation (11) is also applicable for both motors to estimate the stator flux linkage.

$$\bar{\lambda}_s = \int_0^t (\bar{V}_s - r_s \bar{i}_s) dt + \bar{\lambda}_{s|t=0} \quad (11)$$

In which \bar{V}_s and \bar{i}_s are the stator voltage and current space vectors, respectively. In (11), the value of the initial stator flux vector ($\bar{\lambda}_{s|t=0}$) depends on the magnetizing flux PM material.

3.2 Fuzzy Logic Controller

In this section, a simple fuzzy PI (Proportional Integrator) is briefly discussed. Figure 10 shows the schematic of the fuzzy PI, and " $\alpha[n]$ ", the output of the designed controller at time n , is calculated as:

$$\alpha[n] = \alpha[n-1] + \Delta\alpha[n] \quad (12)$$

In (12), " $\Delta\alpha[n]$ " and " $\alpha[n-1]$ " are, respectively, the output of the fuzzy interference and previous value of the controlled signal. The designed fuzzy PI has two inputs, " $e1[n]$ " and " $\Delta e1[n]$ ", and one output " $\Delta\alpha[n]$ ". Three scale factors " $G1$ ", " $G2$ " and " $G3$ " are defined to normalize inputs and denormalize output, respectively. Three triangle functions, depicted in Figure 11,

named "P" (Positive), "Z" (Zero) and "N" (Negative) are defined as the membership functions. Note that the inputs and output membership functions are completely the same. In addition, the input limiters are designed so that the two inputs can be put in the defined range.

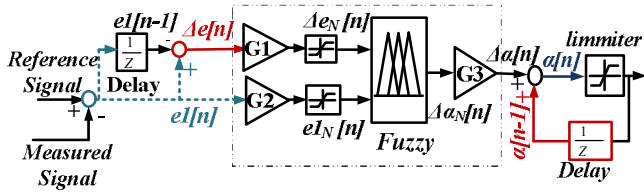


Fig. 10. The schematic of the fuzzy PI controller.

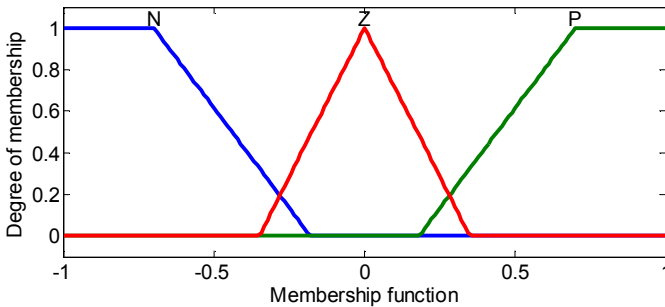


Fig. 11. Degrees of input and output membership functions.

Table 2 shows rules used in fuzzy controller based on this general form: "If ("e" is A) and ("Δe" is B) then output is C". One of the most important advantages of the designed controller is that it does not need any changes for different applications. However, their tunings are necessary. In other words, the same FLCs, tuned based on an optimal response, are employed for torque and flux controllers of both motors, and the value of scale factor parameters is given in Table 3.

Table 2. Rules set for the fuzzy PI controller.

| | | | |
|---|----------|------------|-----------------|
| | <i>e</i> | Δe | $\Delta \alpha$ |
| 1 | Z | Z | Z |
| 2 | P | Z | P |
| 3 | N | Z | N |
| 4 | Z | P | P |
| 5 | Z | N | N |

Table 3. Controller parameters.

| Controller parameters | value |
|---------------------------------------|-------------------|
| sampling time | 20 (us) |
| SVM switching frequency | 5000 (Hz) |
| [G1, G2, and G3] of Flux Controller | [1, 2, and 0.1] |
| [G1, G2, and G3] of Torque Controller | [0.1, 0.2, and 1] |

4. SIMULATION RESULTS

In this section, simulation results of the designed three-phase, 1 (KW), four-pole, 50 (Hz), and 380 (Volt) PMSM and the equal LSPMSM of DTFC-SVM method are provided. In order to present a thorough comparison, not only is the same power system (, i. e. three-phase supply, direct current link, rectifier, and inverter) used but also the same conditions (i.e., the same load torque and flux and torque references) are

tested. In addition, identical fuzzy controllers with the same parameters are designed to evaluate DTC-SVM performance of the PMSM and LSPMSM.

The simulated parameters are listed in Tables 4-5. However, to corroborate the method and verify the operation of LSPMSM and PMSM under DTFC-SVM technique, different conditions are tested. For instance, different reference fluxes and reference torques are tested to support a fan load ($T_L = k\omega_m$). The system has also been discretized with a two-microsecond time step. Stator current of phase "a" ($i_{a\ Stator}$), electromagnetic and reference torques (T_e and $T_{e\ ref}$), motor speed (ω_m), and the stator flux (ϕ_s) of both motors for DTFC-SVM method are presented in Figure 12 and extended in Figures 13-14. For a better comparison, transient and steady-state parameters are also listed in Tables 6 and 7.

Table 4. Machine Parameter.

| Common Electrical Parameters | Common Mechanical Parameters | LSPMSM Parameters |
|------------------------------|----------------------------------|------------------------------|
| $F_n = 50$ (Hz) | $J = 0.002$ (Kg.m ²) | $L'_{lr} = 0.0358$ (H) |
| V_n (RMS L-L) = 380 (V) | $B = 0.00008$ (N.m.s) | $r'_{dr} = 9$ (Ω) |
| $r_s = 10$ (Ω) | $P_n = 750$ (W) | $r'_{qr} = 8.5$ (Ω) |
| $L_{ls} = 0.0358$ (H) | Poles = 4 | $\lambda'_m = 1.32$ |
| $L_{md} = 69.3$ (mH) | $\lambda'_m = 1.32$ (Wb) | |
| $L_{mq} = 0.2597$ (H) | | |

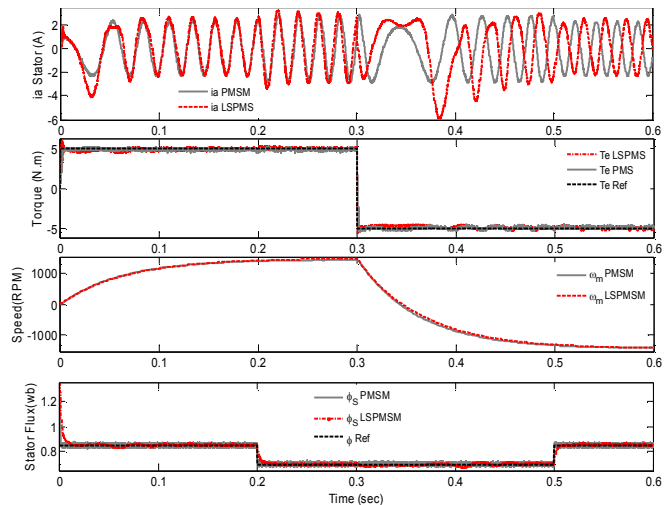


Fig 12. Stator current of phase "a" ($i_{a\ Stator}$), electromagnetic and reference torques (T_e and $T_{e\ Ref}$), motor speeds (ω_m), and the amplitude of stator flux ($|\lambda_s|$) of DTFC-SVM.

Table 5. System Parameters.

| Three-phase Source | Rectifier and DC link | Inverter |
|-------------------------------------|---|--|
| L-L RMS voltage = 380 (V) | Snubber Resistance = 10 (K Ω) Snubber capacitance = 2 (nF) | Snubber Resistance = 10 (K Ω) Snubber capacitance = inf |
| Phase angle of phase A = 0 (Degree) | Device = Diode On-State Resistance = 1 (m Ω) | Device = IGBT/Diode On-State Resistance = 1 (m Ω) [Fall-, tail-] time = [1,2] (us) |

| | | |
|---------------------|---|---|
| Frequency = 50 (Hz) | DC-Bus Capacitance = 7500 (uF) Forward voltage = 1.3 (V) | Forward voltages [IGBT Vf, Diode Vf] = [1.4, 1.4](V) |
|---------------------|---|---|

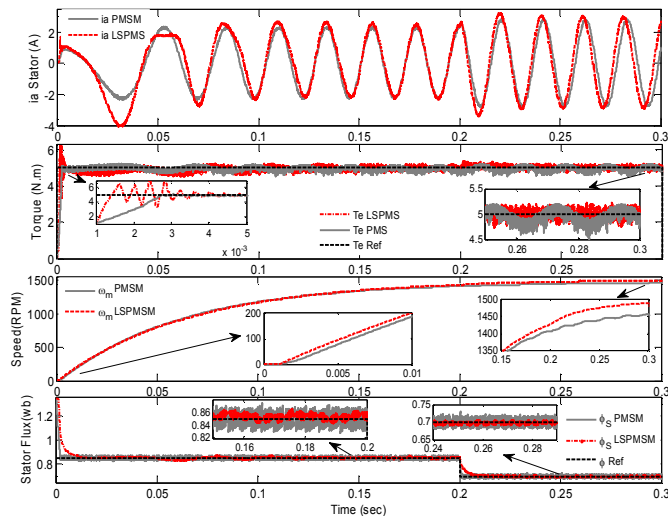


Fig. 13. The extended of Figure 12 in the time interval (0-0.3) seconds (the first and second stages).

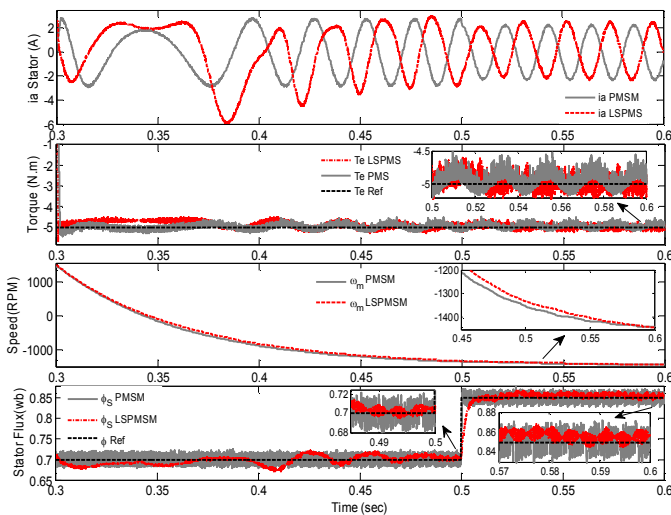


Fig. 14. The extended of Figure 12 in the time interval (0.3-0.6) seconds (the third and fourth stages).

The simulation tests the start-up process of both motors when the reference torque and reference of amplitude of stator flux are equal to 5 (N.m) and 0.85 (Wb), respectively. Simulation results confirm the robustness feature of the designed controller, as both motors are able to provide the reference signals under different conditions. However, Compared to the PMSM, LSPMSM has a better dynamic response, since LSPMSM is able to track instantaneously the reference torque, and consequently the rise time of its electromagnetic torque is lower than that of PMSM, and it shows the superiority of the LSPMSM. It stands to the reason that the operation of LSPMSM in asynchronous region is better than the PMSM, since its rotor windings produce an induction torque. In other words, induction torque of LSPMSM provides its line-starting capability, and this capability causes

a better dynamic response rather than the PMSM. Torque ripple of the LSPMSM is lower than that of the PMSM, since rotor windings operate as damper ones. However, in the steady-state, both motors operate equally, since the rotor induction current and induction torque of LSPMSM for the steady-state can be ignored. Therefore, the stator currents of the steady-state for both motors are the same.

Table 6. Transient and steady-state data obtained from Figures 13.

| | The First Stage (0-0.2) Second | | The Second Stage (0.2-0.3) Second | |
|---|--------------------------------|---------|-----------------------------------|---------|
| Electrical Machinery | PMSM | LS PMSM | PMSM | LS PMSM |
| Rise Time for Torque Control (Sec.) | 0.0026 | 0.0014 | - | - |
| Torque Ripple in S-S (N.m) | 0.6 | 0.25 | 0.5 | 0.15 |
| Rise Time for Flux control (Sec.) | 0.025 | 0.007 | 0.0015 | 0.005 |
| Flux Ripple in S-S (Wb) | 0.04 | 0.025 | 0.035 | 0.018 |
| Stator current P-P in the First Cycle (A) | 3.3 | 6 | 5.4 | 6.65 |
| THD of Stator Current in S-S (%) | 7 | 6.95 | 7.6 | 7.2 |
| Fundamental Component in S-S (A) | 2.32 | 2.35 | 2.8 | 2.85 |
| Efficiency in S-S (%) | 92 | 91.8 | 84.9 | 84.9 |
| PF in S-S | 0.71 | 0.71 | 0.71 | 0.69 |

It is obvious that, for low speeds, rotor windings of the LSPMSM cause an inductive behaviour. For this reason, as shown in Figure 13, the starting current of the LSPMSM is higher than that of the PMSM. In addition, for a classical switching table DTFC, the torque ripple of LSPMSM in low speed region is higher than that of the PMSM, due to induction behaviour of the LSPMSM. Nevertheless, as it is expected, the DTFC-SVM method is effective to reduce the torque ripple of the LSPMSM especially in the low speed region.

To assess the effect of the stator flux, at 0.2 (sec), the reference flux is changed from 0.85 to 0.7 (Wb). It should be noted that reducing the reference flux increases the stator current. DTFC-SVM technique significantly reduces the fluctuations of induction torque of the LSPMSM, and it results a reduced electromagnetic torque ripple and speed vibrations rather than PMSM. The LSPMSM which features low torque and flux ripple in the most operating conditions operates even better than PMSM. Damping the induction torque in the steady-state, both motors operate almost equally. For instance, their efficiency, THD of the stator current, fundamental component of the stator current, and PF in the steady-state are approximately the same.

Table 7. Transient and steady-state data obtained from Figures 14.

| Electrical Machinery | The Third Stage (0.3-0.5) Second | | The Fourth Stage (0.2-0.3) Second | |
|---|----------------------------------|---------|-----------------------------------|---------|
| | PMSM | LS PMSM | PMSM | LS PMSM |
| Rise Time for Torque Control (Sec.) | 0.0018 | 0.001 | - | - |
| Torque Ripple in S-S (N.m) | 0.5 | 0.5 | 0.6 | 0.25 |
| Rise Time for Flux control (Sec.) | - | - | 0.0008 | 0.005 |
| Flux Ripple in S-S (Wb) | 0.04 | 0.02 | 0.04 | 0.025 |
| Stator current P-P in the First Cycle (A) | 5.75 | 5.5 | 4.9 | 4.95 |
| THD of Stator Current in S-S (%) | 6.5 | 6.51 | 7.81 | 7.82 |
| Fundamental Component in S-S (A) | 2.9 | 2.93 | 2.3 | 2.34 |
| Efficiency in S-S (%) | 82.6 | 82.5 | 91 | 90.53 |
| PF in S-S | 0.68 | 0.68 | 0.76 | 0.77 |

After stabilizing motors at the steady-state speed, at $t = 0.3$ (s), the reference torque and consequently the generated electromagnetic torques are inverted abruptly, passing from 5 (N.m) to -5 (N.m), and the electromagnetic torque is decreased. Therefore, the rotor speed signal decreases from a positive value to a negative one, due to the fan load. As shown in Figures 13-14, both motors are able to follow the flux and torque references in both directions. Figures 13-14 also report that the main drawback of the LSPMSM, which is its high torque ripples in the low speed region, is removed even for the negative reference torque, thanks to the fixed switching frequency of the DTFC-SVM method. Finally, to evaluate different conditions, the reference flux value is changed from 0.7 to 0.85 (Wb). Again, Figure 14 confirms the proposed superiority of the LSPMSM against the PMSM, due to the lower flux and torque ripples and better dynamic responses.

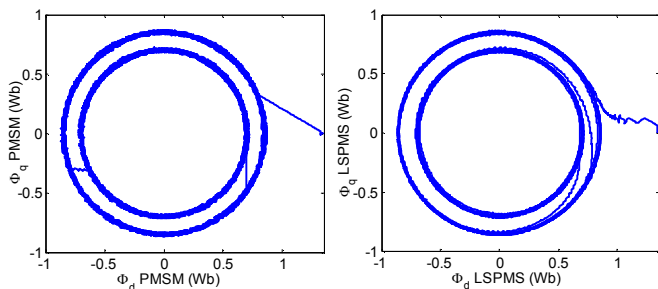


Fig. 15. The stator flux locus of direct and quadratic axes.

In general, the rotor losses of the LSPMSM and induction torque slightly increase its stator current and apparent power rather than the PMSM, and the rotor windings have a repercussion on the motor efficiency. Even though, the designed fuzzy controllers operate as well, the torque and

flux controllers affect the overall performance of the aforementioned machines. Therefore, even a better response for the LSPMSM and PMSM can be obtained, if the fuzzy controllers are optimized using neural networks, adaptive neural fuzzy interface system, or scheduling gains.

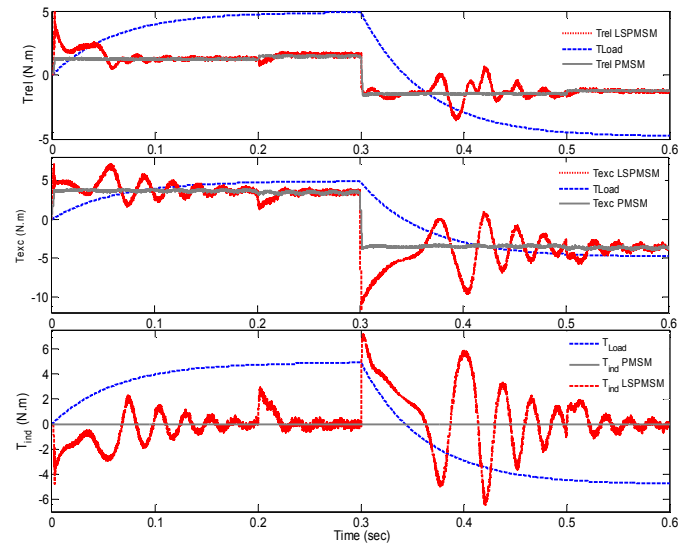


Fig. 16. Load torque (T_{Load}) and torque Components of the LSPMSM and PMSM for DTFC-SVM method shown in Figure 12.

In general, the rotor losses of the LSPMSM and induction torque slightly increase its stator current and apparent power rather than the PMSM, and the rotor windings have a repercussion on the motor efficiency. Even though, the designed fuzzy controllers operate as well, the torque and flux controllers affect the overall performance of the aforementioned machines. Therefore, even a better response for the LSPMSM and PMSM can be obtained, if the fuzzy controllers are optimized using neural networks, adaptive neural fuzzy interface system, or scheduling gains.

In order to present an in-depth comparison, the stator flux locus for both motors of direct and quadratic axes is also shown in Figure 15. It highlights the superiority of the LSPMSM rather than the PMSM as well, since the LSPMSM stator flux has a lower ripple rather than that of PMSM.

Torque components of both motors and load torque (T_{Load}) are shown in Figure 16. Excitation and reluctance torque ripples of the LSPMSM are significantly higher than those of PMSM. Nevertheless, the interaction of induction torque between the other torque components of LSPMSM reduces the overall torque ripple of LSPMSM and speed variations, since the rotor windings of LSPMSM operate as damper ones. In addition, T_{exc} and T_{rel} of the LSPMSM in the transient state are higher than those of PMSM, due to the adverse effect of induction torque. It results a superior dynamic response of LSPMSM rather than PMSM, and their steady-state response are approximately the same, since there is no induction torque for the synchronous speed. It should be noted that the induction torque of the LSPMSM increases starting current of LSPMSM. For this reason the starting current of the LSPMSM is higher than that of PMSM.

5. CONCLUSION

In this paper, a simple and well-known DTFC based on SVM technique is designed for LSPMSM, and it is compared with the same PMSM. The high performance of the DTFC-SVM method indicates the possibility for the replacement of IMs and PMSMs with LSPMSMs in the electrical drive applications, and LSPMSM performance would be more improved if fuzzy controllers were optimized through neural networks. For this purpose, further research might evaluate LSPMSM performance by an experimental method.

6. ABBREVIATIONS

LSPMS: Line-Start Permanent Magnet Synchronous Motor
 IM: Induction Motor
 PM: Permanent Magnet
 (d - q - 0) axes: direct, quadratic, and zero axes
 DTFC: Direct Torque Control
 PMSM: Permanent Magnet Synchronous Motor
 THD: Total Harmonic Distortion
 PF: Power Factor
 RMS: Root Mean Square
 L-L: Line-to-Line
 S-S: Steady-State
 FLC: Fuzzy Logic Controller
 PI: Proportional Integrator
 (P, Z, N): Positive, Zero, and Negative
 SVM: Space vector Modulated.

7. SYMBOLS

(V_{ds} , V_{qs}): the stator voltage of d-q axes.
 (i_{ds} , i_{qs}): the stator current of d-q axes.
 (λ_{ds} , λ_{qs}): and stator flux of d-q axes.
 (V'_{dr} , V'_{qr}): rotor voltage of d-q axes referred to stator side.
 (i'_{dr} , i'_{qr}): the rotor current of d-q axes referred to stator side.
 (λ'_{dr} , λ'_{qr}): the rotor flux of d-q axes referred to stator side.
 (V_{0s} , i_{0s} , λ_{0s}): the stator voltage, current, and flux of zero sequence.
 (V'_{0r} , i'_{0r} , λ'_{0r}): the rotor voltage, current and flux of zero sequence referred to stator side.
 (r_s , L_{ls}): the stator resistance, the stator leakage- inductance.
 (r'_r , L'_{lr}): the rotor resistance and leakage- inductance referred to the stator side.
 ω_m : the angular motor speed.
 (P , p): the pole numbers and the derivative operator.
 (T_e , T_{Load}): the electromagnetic and load torques.
 (B , J): the friction coefficient and moment of inertia.
 (L_{md} , L_{mq}): the magnetizing inductance of d-q axes.
 (r'_{qr} , r'_{dr}): the rotor resistance of d-q axes referred to the stator side.
 (λ'_m , i'_m): the magnetizing flux and current of the PM referred to the stator side.
 (\bar{V}_s , $\bar{\lambda}_s$, and \bar{i}_s): Stator voltage, flux-linkage, and current space vectors.
 $\bar{\lambda}_{s|t=0}$: The initial stator flux-linkage space vector.
 (e_T and e_λ): the torque and flux error signals.
 ($T_{e\ ref}$ and $T_{e\ est}$): the reference and estimated torque signals.
 ($|\lambda_{s\ est}|$, $|\lambda_{s\ ref}|$): the magnitude of estimated and reference stator fluxes.

(S_1 , S_2 ... and S_6): the flux sectors.
 (V_0 , V_1 ... and V_7): the inverter output voltage space vectors
 $i_{a\ Stator}$: the stator current of phase "a".
 (T_{exc} , T_{Rel} , and T_{ind}): Excitation, reluctance, and induction torques.
 ($eI [n]$, $\Delta eI [n]$): error signal and variation of error signal of the designed fuzzy controller at time n.
 $\Delta \alpha [n]$: variation of FLC output.
 (G_1 , G_2 , and G_3): Three scale factors of the designed fuzzy controller.
 (V_{qs}^* , V_{ds}^*): the reference value of the quadrature and direct axes stator voltage.
 f_s : Switching frequency.
 (\bar{V}_a , \bar{V}_b): two nearest active vectors.
 α : the angle between \bar{V}_a and \bar{V}_s vectors.
 \bar{V}_s : the reference vector in SVM technique.
 (T_0 , T_1 , and T_2): time duration of zero and two nearest active vectors in SVM technique.

REFERENCES

- CheeMun O. Dynamic simulation of electric machinery. New Jersey, PTR: Prentice Hall, 1997.
 deAlmeida AT, Ferreira FJTE, Fong JAC, Standards for efficiency of electric motors, *Ind. Appl. Mag IEEE* 2011; 17: 12-19.
 Elbadi B., Bouzidi B., Masoudi A., DTC scheme for a four-switch inverter-fed induction motor emulating the six-switch inverter operation, *Pow Elec. IEEE Trans* 2013; 28: 3528-3538.
 Fei W., Luk P., Ma J., Shen J.X., Yang G., A high-performance line-start permanent magnet synchronous motor amended from a small industrial three-phase induction motor, *Mag. IEEE Trans* 2009; 45: 4724-4727.
 Ferreira FJTE, Fong JAC, deAlmeida AT, Ecoanalysis of variable-speed drives for flow regulation in pumping systems, *Ind Elect IEEE Trans* 2011; 58: 2117-2125.
 Isfahani A.H., Vaez-Zadeh S., Line-start permanent magnet synchronous motors: challenges and opportunities, *Energy* 2009; 34: 1755-1763.
 Jidin A.B., Idris NRBN., Yatim AHBM., Elbuluk M.E., Sutikno T., A wide speed high torque capability utilizing over modulation strategy in DTC of induction machines with constant switching frequency controller, *Po. Elect. IEEE Trans* 2012; 27: 2566-2575.
 Kahrisangi M.G., Isfahani A.H., Vaez-Zadeh S., Sebdani M.R., Line-start permanent magnet synchronous motors versus induction motors: a comparative study, *Front Elect. & Elect. Eng*; 2012; 7: 1-8.
 Kurihara K., Rahman M.A., High-efficiency line-start interior permanent-magnet synchronous motors, *Ind. Appl. IEEE Trans* 2004; 40: 789-796.
 Marcic T., Stumberger B., Stumberger G, Comparison of induction motor and Line-Start IPM Synchronous Motor performance in a variable-speed drive, *Ind. Appl. IEEE Trans* 2012; 48: 2341-2352.
 Marcic T., Stumberger B., Stumberger G., Hadziselimovic M., Virtic P., Dolinar D., Line-starting three- and single-phase interior permanent magnet synchronous motors-direct comparison to induction motors, *Mag. IEEE Trans*

- 2008; 44: 4413-4416.
- Melfi M., Evon S., McElveen R., Induction versus permanent magnet motors, *Ind. Appl. Mag IEEE* 2009; 15: 28-35.
- Melfi MJ., Rogers SD., Evon S., Martin B., Permanent-magnet motors for energy savings in industrial applications, *Ind. Appl. IEEE Trans* 2008; 44: 1360-1366.
- Schwartz D.G., Klir G.J., Lewis H.W., Ezawa Y., Application of fuzzy sets and approximate reasoning, *Syst. IEEE Trans* 1994; 82: 482-498.
- Stumberger B., Marcic T., Hadziselimovic M., Direct comparison of induction motor and line-start IPM synchronous motor characteristics for semi-hermetic compressor drives, *Ind. Appl. IEEE Trans* 2012; 48: 2310-2321.
- Taravat S., Niasar A.H., Rabiee A, Sensor less vector control of single phase line start permanent magnet motors (LSPMs), *Int. J. Sci. & Adv Tech* 2012; 2: 126-131.
- Uddin M.N., Hafeez M., FLC-Based DTC scheme to improve the dynamic performance of an IM drive, *Ind. Appl. IEEE Trans* 2012; 48: 823-831.
- Vas P, Sensor less vector and direct torque control, Oxford and New York, UK: *Oxford university press*, 1998.
- Yongchang Z., Jianguo Z., Direct torque control of permanent magnet synchronous motor with reduced torque ripple and commutation frequency, *Po. Elect. IEEE Trans* 2011; 26: 235-248.
- Yongchang Z., Jianguo Z., Zhengming Z., Wei X., Dorrell D.G., An improved direct torque control for three-level inverter-fed induction motor sensor less drive, *Po. Elec. IEEE Trans* 2012; 27: 1502-1513.